JACS
JOURNAL OF THE AMERICAN CHEMICAL SOCIETY

Article

pubs.acs.org/JACS

Sequence, Structure, and Function of Peptide Self-Assembled Monolayers

Ann K. Nowinski, Fang Sun, Andrew D. White, Andrew J. Keefe, and Shaoyi Jiang*

Department of Chemical Engineering, University of Washington, Seattle, Washington 98195, United States

Supporting Information

ABSTRACT: Cysteine is commonly used to attach peptides onto gold surfaces. Here we show that the inclusion of an additional linker with a length of four residues (-PPPPC) and a rigid, hydrophobic nature is a better choice for forming peptide self-assembled monolayers (SAMs) with a well-ordered structure and high surface density. We compared the structure and function of the nonfouling peptide EKEKEKE-PPPPC-Am with EKEKEKE-C-Am. Circular dichroism, attenuated total internal reflection Fourier transform IR spectroscopy, and molecular dynamics results showed that EKEKEKE-PPPPC-Am forms a secondary structure while EKEKEKE-C-Am has a random structure. Surface plasmon resonance sensor results showed that protein adsorption on EKEKEKE-PPPPC-Am/gold is very low with small variation while protein adsorption on EKEKEKE-C-Am/gold is high with large variation. X-ray photoelectron spectroscopy results showed that both peptides have strong gold−thiol binding with the gold surface, indicating that their difference in protein adsorption is due to their assembled structures. Further experimental and simulation studies were performed to show that -PPPPC is a better linker than -PC, -PPC, and -PPPC. Finally, we extended EKEKEKE-PPPPC-Am with the cell-binding sequence RGD and demonstrated control over specific versus nonspecific cell adhesion without using poly(ethylene glycol). Adding a functional peptide to the nonfouling EK sequence avoids complex chemistries that are used for its connection to synthetic materials.

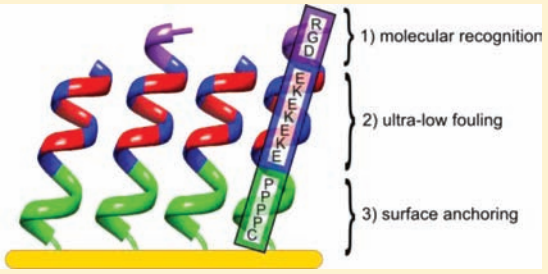

INTRODUCTION

A nonfouling peptide was formed by alternating negatively charged glutamic acid (E) and positively charged lysine (K) amino acid residues.[1] This corresponds with our recent analysis of many protein surfaces, which indicated that E and K are the two most prevalent amino acids on the surfaces of proteins. The EK sequence forms a strong hydration layer similar to that in zwitterionic materials.[2] Natural materials based on nonfouling peptides have many biomedical applications. A nonpeptide synthetic thiol anchor[1,3,4] is often used to attach functional peptides to gold surfaces. Polypeptide mimics have also been used as water-resistant anchors to surfaces and display fouling resistance.[5] EK peptide-based self-assembled monolayers (SAMs) containing synthetic butanethiol anchors have previously been shown to have high surface packing densities and ultra-low fouling properties on gold surfaces.[1] It is, however, highly desirable to replace these synthetic linkers with a natural peptide for surface attachment to form an all-peptide-based material. The amino acid cysteine (C), which contains a thiol side chain,[6]has commonly been used to attach peptides onto gold surfaces. Although cysteine binds strongly to gold, unlike synthetic thiol anchors, a peptide using cysteine alone as its surface anchoring group was not able to achieve the well-ordered structure and high surface density necessary for ultra-low fouling surfaces.[7]

In addition to low fouling properties, it is beneficial to achieve specific interactions for biomedical applications. One such application is mimicking extracellular matrix proteins using the well-established arginine-glycine-aspartate (RGD) sequence, which can mimic fibronectin, vitronectin, fibrinogen, osteopontin, and bone sialoprotein.[8] This and other functional sequences are commonly conjugated onto a nonfouling synthetic polymer such as poly(ethylene glycol) (PEG)[9] to prevent nonspecific protein adsorption, which can undermine sequence specificity. Such conjugation processes are complex.[10] Polydispersity of the polymers, identification of appropriate conjugation sites, nonuniformly distributed functional groups, and difficult postconjugation evaluation[11,12] are all drawbacks to various conjugation methods. Integrating the nonfouling EK peptide sequence with RGD allows the replacement of nonfouling synthetic materials and avoids the complex chemistries used in bioconjugation.

In this work, we investigated the impact of the length and the nature of a short linker to form a well-packed, ultra-low fouling peptide SAM. Specifically, this involved the inclusion of one to four additional proline linker residues, which provide hydrophobicity and helical secondary structure. We compared the structures of the nonfouling sequence EKEKEKE-PPPPC-Am and EKEKEKE-C-Am in solution and on a gold surface. The low fouling segment of the peptide contains four negative glutamic acid residues (E) and three positive lysine residues (K). Overall charge neutrality of the peptide is maintained by leaving the N-terminus as a free amine, which contributes an

Received: January 20, 2012
Published: March 8, 2012

   dx.doi.org/10.1021/ja3006868 | J. Am. Chem. Soc. 2012, 134, 6000−6005

extra positive charge to the peptide. The C-termini of all of the peptides were amidated to cap the negative charge of the carboxylic acid, which could create a negative charge near the gold-binding thiol that might impede packing of the SAM through electrostatic repulsion.

The secondary structures of these two sequences were characterized using circular dichroism (CD) and attenuated total internal reflection Fourier transform IR spectroscopy (ATR-FTIR) in solution and on the surface, respectively. Molecular dynamics (MD) simulations were also performed to elucidate the secondary structure differences further. X-ray photoelectron spectroscopy (XPS) was used to evaluate surface attachment. Nonspecific protein adsorption was measured via surface plasmon resonance (SPR) sensors. Furthermore, RGD was added to the N-terminus of the EKEKEKE-PPPPC-Am sequence to gain specific cell adhesion against an ultra-low fouling background of the EK peptide, eliminating the need for conjugation of biomolecular recognition peptides to nonfouling synthetic polymers such as PEG. The peptide sequence RGD-EKEKEKE-PPPPC-Am used in this work is illustrated in Figure 1. This all-in-one peptide contains biomolecular recognition, ultra-low fouling, and surface anchoring functions.

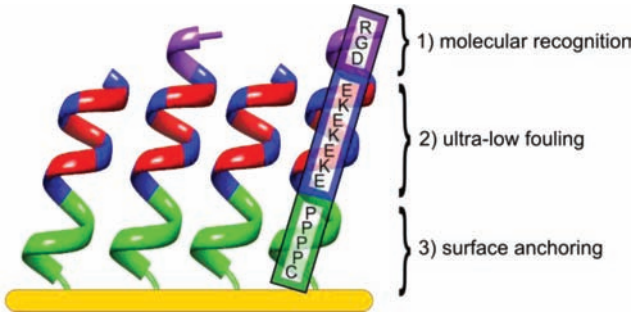

Figure 1. All-in-one natural peptide SAM on gold with three distinct functions incorporated into the peptide sequence: (1) biomolecular recognition via RGD; (2) ultra-low fouling via EK; and (3) surface anchoring via a linker composed of four rigid, hydrophobic proline (P) residues and a cysteine (C) residue and having a secondary structure, to achieve a well-ordered structure and high surface density.

RESULTS AND DISCUSSION

Impact of the Nature and Length of the Linker on SAM Formation. SPR results show that simply using a cysteine residue containing a thiol side chain for surface anchoring is insufficient to form a low fouling peptide SAM (Figure 2a). The fouling to fibrinogen and lysozyme for the linker-free peptide SAM (EKEKEKE-C-Am) is 38.3 ± 29.0 and 5.3 ± 4.4 ng/cm^2, respectively. In addition to high fouling, there is a large distribution in the fibrinogen protein adsorption values (Figure 2b).

Here we considered the effect of including a proline (P) linker and a glycine (G) linker in the EKEKEKE-C-Am peptide. Proline was selected on the basis of its hydrophobicity, its ability to act as an α-helix-destabilizing residue,[13] and its rigid structure, all of which should promote packing for SAM formation. Additionally, the covalently constrained backbone of proline reduces the entropy loss upon adsorption of the peptide to the surface, whereas other amino acids lose mobility upon adsorption.[14] Glycine was selected on the basis of its hydrophilicity and its flexibility for comparison with proline.

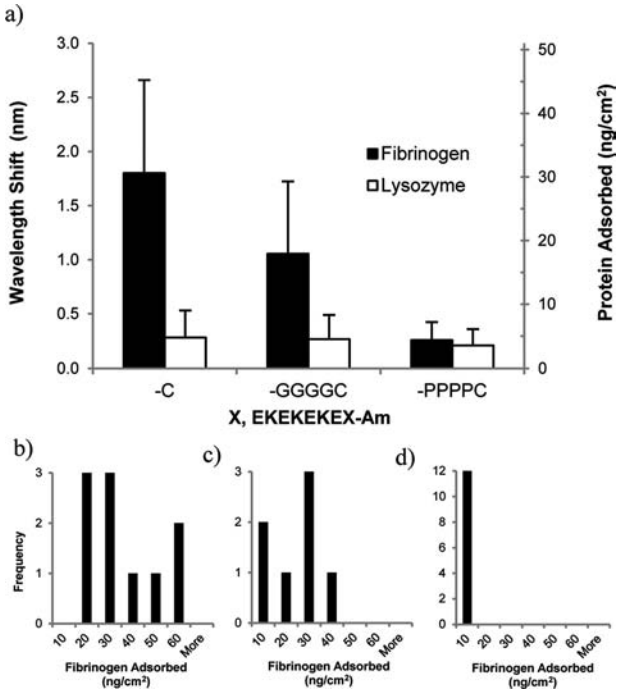

Figure 2. (a) Protein adsorption on peptide SAMs composed of the linker-free peptide (EKEKEKE-C-Am), the glycine linker peptide (EKEKEKE-GGGGC-Am), and the proline linker peptide (EKEKEKE-PPPPC-Am). SPR results for fibrinogen (black) and lysozyme (white) are in the unit of wavelength shift (nm) or converted surface concentration (ng/cm^2). Each data point represents an average value ± standard deviation from at least three independent measurements. (b–d) Histograms of adsorbed fibrinogen protein (ng/cm^2) for (b) linker-free peptide, (c) glycine linker peptide, and (d) proline linker peptide.

The additional inclusion of four prolines as a linker resulted in an ultra-low fouling SAM, defined as having a fibrinogen adsorption of less than 5 ng/cm^2.[15] The fouling to fibrinogen and lysozyme for the proline linker peptide SAM (EKEKEKE-PPPPC-Am) is 4.4 ± 2.9 and 3.5 ± 2.6 ng/cm^2, respectively, which is comparable to the previously studied butanethiol-containing peptide SAM.[1] Furthermore, the proline linker peptide has a narrow distribution for fibrinogen protein adsorption, as opposed to the large distribution seen for the linker-free peptide (Figure 2d).

For comparison with the rigid, hydrophobic proline residue, the flexible, hydrophilic glycine residue was also used as a linker. SPR results indicate that the inclusion of a glycine linker (EKEKEKE-GGGGC-Am) results in a high fouling SAM, with fouling to fibrinogen and lysozyme of 17.9 ± 11.4 and 4.5 ± 3.8 ng/cm^2, respectively. It is not surprising that the flexible linker compromised the fouling properties of the SAM, as this would disrupt close packing on the surface, just as in the linker-free peptide. The glycine linker peptide also has a large distribution for fibrinogen protein adsorption (Figure 2c). In contrast, the inclusion of the rigid, hydrophobic proline linker allows for favorable hydrophobic interactions between chains, enabling better packing. These hydrophobic groups may play a role analogous to that of the methyl groups found in synthetic butanethiol anchors.[1]

To determine how many linker residues are needed to promote close packing of the surface, the effect of linker length on the fouling properties of the SAMs was examined. Backbone

dx.doi.org/10.1021/ja3006868 | J. Am. Chem. Soc. 2012, 134, 6000–6005

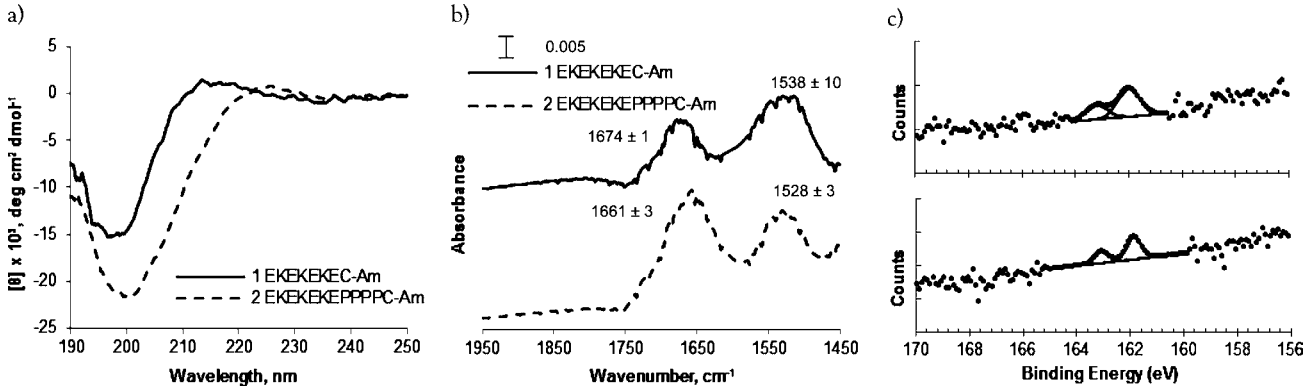

Figure 3. Comparison of the secondary structures of the linker-free peptide (EKEKEKE-C-Am) and the proline linker peptide (EKEKEKE-PPPPC-Am). (a) CD spectra of peptide sequences EKEKEKE-C-Am (1, solid) and EKEKEKE-PPPPC-Am (2, dashed) in 10 mM potassium phosphate, 50 mM sodium sulfate buffer (pH 7.4). (b) Representative ATR-FTIR spectra for the peptide SAMs EKEKEKE-C-Am (1, solid) and EKEKEKE-PPPPC-Am (2, dashed) on Au(111)-coated mica substrate. The average maximum intensities from at least three independent measurements for (left) amide I and (right) amide II bands are listed above the peaks in the spectrum. (c) XPS S 2p spectra for EKEKEKE-C-Am (top) and EKEKEKE-PPPPC-Am (bottom) peptide SAMs adsorbed on a Au(111)-coated mica substrate. To properly fit the experimental peptide SAM spectrum, a S 2p doublet with a 2:1 area ratio and a splitting of 1.2 eV was used.

and side-chain Monte Carlo simulations were performed using the Rosetta scoring function[16] on peptide sequences containing one to four prolines in the linker. These simulations predict peptide conformations in solution. Because these peptides contain so few residues, they lack a deep free energy minimum (fold) and are expected to shift between several low-energy conformations. A sample of the lowest-energy structures predicted by simulations for peptide sequences containing one to four prolines in the linker shows that the addition of proline favors an extended, rigid conformation for the peptide sequence (Figure S1 in the Supporting Information). We hypothesize that the extended, rigid conformation allows for closer packing of peptide chains, thus enabling the formation of a uniform, low fouling surface. As expected, SPR results indicate that an increase in the number of prolines corresponds to a decrease in the amount of adsorbed protein (Figure S1). The linker containing four prolines is the threshold for achieving an ultra-low fouling surface, and thus, the linker length was chosen to be four peptide residues. Overall, simply using a cysteine residue for surface anchoring does not provide a peptide capable of self-assembly into an ultra-low fouling surface. Thus, selection of an appropriate peptide linker that allows close packing of chains is essential. Here we have identified a linker having a length of four residues and a rigid, hydrophobic nature as one possible robust option. Other strategies have been considered using natural peptides to improve peptide self-assembly on surfaces,[17] on nanoparticles,[18] and for membrane formation.[19]

Impact of Secondary Structure on SAM Formation. To investigate further the large differences in fouling between the linker-free peptide (EKEKEKE-C-Am) and the proline linker peptide (EKEKEKE-PPPPC-Am), we examined the secondary structure in solution via CD and MD simulations and on the surface via ATR-FTIR. CD spectra were collected in 10 mM potassium phosphate, 50 mM sodium sulfate buffer (pH 7.4) (Figure 3a). The CD spectrum for the linker-free peptide is indicative of a disordered structure with very low ellipticity above 210 nm and negative bands near 195 nm.[20] In contrast, the CD spectrum for the proline linker peptide designates an extended polyproline helix conformation with a strong negative band near 200 nm and a weaker positive band around 225 nm.[21]

Replica-exchange MD simulations in solution were performed to supplement the CD data for the linker-free peptide, the proline linker peptide, and the glycine linker peptide. The top panel of Figure 4 shows the lowest-energy secondary structure at each residue position for the three peptides. The linker-free and glycine linker peptides lack secondary structure. The proline linker peptide displays a helical structure, most likely due to the rigidity imparted to the backbone by the proline linker. The bottom panel of Figure 4 shows the Cα-to-Cα end-to-end distances of the peptides as probability

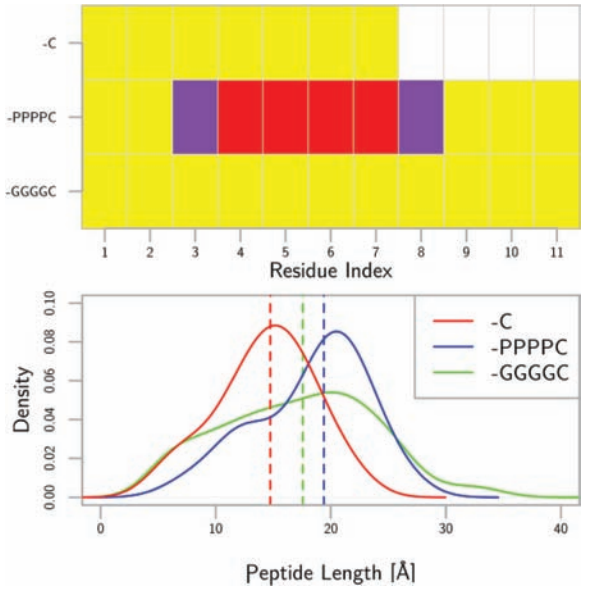

Figure 4. (top) Secondary structure mode for each residue on the three different peptides. The secondary structure was determined using the DSSP program on the trajectories obtained from tempered-annealing MD simulations of dilute peptides. Yellow indicates no secondary structure, purple a turn or bend with a hydrogen bond, and red an α-helix. (bottom) Probability distributions of the Cα-to-Cα distance between the initial and final residues in the peptide. The probability distributions were taken from a kernel density estimator with a bandwidth of 3. The vertical lines are the medians of the data. The proline linker peptide is the most extended of the three.

dx.doi.org/10.1021/ja3006868 | J. Am. Chem. Soc. 2012, 134, 6000−6005

distributions, with the vertical lines showing the medians. The proline linker peptide is indeed more extended than both the linker-free and the glycine linker control peptides.

We examined the linker-free and proline linker peptide SAMs on a gold surface using ATR-FTIR. Evaluation of ATR-FTIR amide I bands provides surface-sensitive information about the secondary structure of peptide monolayers. The ATR-FTIR spectrum for the linker-free peptide resulted in maximum intensities for amide I and amide II bands at 1674 ± 1 and 1538 ± 10 cm^{-1}, whereas the ATR-FTIR spectrum for the proline linker peptide resulted in maximum intensities for amide I and amide II bands at 1661 ± 3 and 1528 ± 3 cm^{-1} (Figure 3b). The higher-wavenumber peak of the amide I band for the linker-free peptide at 1674 cm^{-1} is not characteristic of an α-helix or a β-sheet, suggesting that the structure of this peptide is disordered.[22,23] The amide I band for the proline linker peptide at 1661 cm^{-1} is shifted to slightly higher wavenumber than regular α-helical structures, which typically have amide I bands at 1650−1658 cm^{-1}. This most likely represents the presence of distorted and/or 3_{10} helices, as expected for a peptide containing several proline residues.[24] Furthermore, the major amide I band is considerably broad, indicating a larger distribution of slightly different helical structures.

The CD, MD, and ATR-FTIR results all support a disordered, random structure for the linker-free peptide and an extended, helical structure for the proline linker peptide. This secondary structure characterization provides a possible explanation for the differences in fouling for the two surfaces. The disordered structure of the peptide containing no linker (EKEKEKE-C-Am) could impede packing of the peptide SAM, resulting in nonuniform surface coverage that would lead to high fouling and large variations in the results. At the same time, the defined, extended conformation of the proline linker peptide (EKEKEKE-PPPPC-Am) allows for closer packing of the monolayer and a more uniform surface with consistent ultra-low fouling behavior. These results indicate that it is preferable to have a well-defined secondary structure to form a closely packed, uniform monolayer.

Finally, XPS data were collected for the linker-free and proline linker peptide SAMs to confirm that the difference in their performance is due to their secondary structure rather than their surface binding characteristics. The binding energy of the S $2p_{3/2}$ peak was 161.9 eV for both surfaces, consistent with sulfur atoms bound to the gold surface as a thiolate species (Figure 3c).[25] The presence of only bound thiolate species in the high-resolution sulfur spectra indicate that the thiol side chain of the cysteine anchor is bound to the gold and is not simply physically adsorbed on the surface. XPS data also provide information about the surface coverage and lateral packing density of a SAM, as determined by measurement of the attenuation of the metal substrate photoelectrons (Au 4f).[26] The gold signal for the proline linker peptide is lower than the gold signal for the linker-free peptide, indicating that the proline linker peptide SAM surface is more densely packed (Figure S2 in the Supporting Information). However, the longer length of the proline linker peptide relative to the linker-free peptide may also partially account for the attenuation of the gold signal. The higher surface coverage of the proline linker peptide SAM indicates improved packing of the peptide chains, corroborating the secondary structure data from CD, MD, and ATR-FTIR.

Several parameters influence the monolayer architecture and thus the low fouling behavior, including chemical moieties, secondary structure formation, peptide length, and peptide packing density. The inclusion of the linker containing four proline residues introduced in this work induces a helical structure at the base of the peptide, as evidenced by ATR-FTIR and MD simulations. The helical formation reduces the mobility of the chains. Thus, this rigid secondary structure results in more uniform peptide molecular conformations, allowing chains to pack tighter, increasing the packing density and reducing fouling. As shown in Figure S1 in the Supporting Information, the number of proline residues in the linker has a profound effect on fouling because of its importance in maintaining the rigid structure necessary for well-packed monolayers. The transition from three to four proline residues, however, shows that the effect of the peptide length lessens beyond three linker residues. Similarly, as shown in Figure 4, the EK residues more than four units beyond the linker are no longer influenced, adopting the random conformations seen in the linker-free and glycine linker sequences. Unlike mixed-charge alkanethiol SAMs, where regular crystalline structures are observed,[1] we expect that the solvent-exposed surface of peptide SAMs is a uniform display of mixed-charge E and K residues. Our previous work on mixed E and K random coplymerization[1] showed that even with amorphous conformations, nonfouling is achieved.

Specific Biomolecular Recognition on an Ultralow-Fouling Background. In this experiment, we extended EKEKEKE-PPPPC-Am with the cell-binding sequence RGD. Cell adhesion onto peptide SAMs composed of mixtures of RGD-EKEKEKE-PPPPC-Am and EKEKEKE-PPPPC-Am was evaluated to display the biomolecular recognition capabilities of our all-in-one peptide biomaterial. The molar percentage of RGD-EKEKEKE-PPPPC-Am was increased from 0 to 100%. Peptide SAMs were seeded with NIH-3T3 fibroblast cells and incubated in supplemented medium for a period of 24 h and then evaluated for cell adhesion by phase-contrast microscopy. As expected, the number of adhered cells increased proportionally to the molar percentage of the RGD-EKEKEKE-PPPPC-Am peptide (Figure 5). The SAM composed entirely of EKEKEKE-PPPPC-Am had no cell attachment, corresponding to the ultra-low fouling results for protein adsorption. The scrambled sequence RDG-EKEKEKE-PPPPC-Am was mixed with EKEKEKE-PPPPC-Am at molar percentages of 50% and 75% and evaluated for cell adhesion as a control. Surfaces containing scrambled RDG showed significantly less cell adhesion than peptide SAMs containing RGD (Figure S3 in the Supporting Information). Furthermore, cells adhering to the scrambled RDG surfaces displayed rounded morphology, whereas cells adhering to RGD surfaces were well spread out. These results show that interactions seen for the RGD sequence are specific and that the EK portion of the peptide maintains an ultra-low fouling background.

■ CONCLUSIONS

Overall, simply using a cysteine residue for surface anchoring does not provide a peptide capable of self-assembly into an ultra-low fouling monolayer on gold surfaces. Selection of an appropriate peptide linker that allows close packing of the chains is essential. Here we have identified a linker consisting of four proline residues together with the amino acid cysteine and having a rigid, hydrophobic nature as one possible robust linker. This provides a well-defined secondary structure needed to promote closely packed monolayers with ultra-low fouling properties. The -PPPPC linker is an effective surface-anchoring

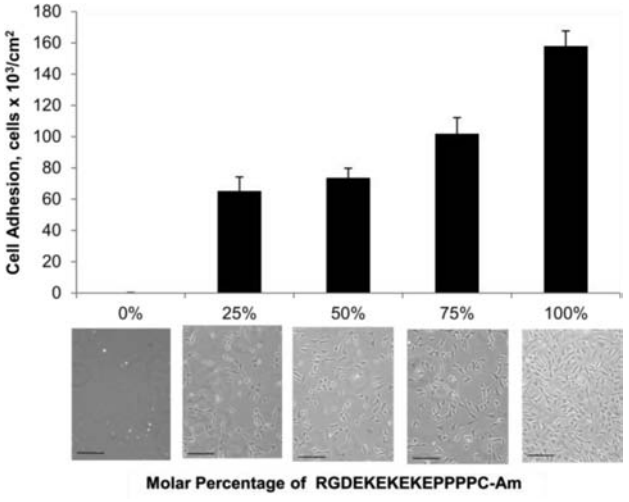

Figure 5. Cell adhesion results after incubation for 24 h in supplemented medium for peptide SAMs composed of mixtures of RGD-EKEKEKE-PPPPC-Am and EKEKEKE-PPPPC-Am. The molar percentage of RGD-EKEKEKE-PPPPC-Am was increased from 0 to 100%. The scale bar represents 100 μm. Cell adhesion for the scrambled peptide sequence RDG-EKEKEKE-PPPPC-Am was evaluated as a control (see the Supporting Information).

sequence for a wide range of applications beyond nonfouling involving peptide assembly onto a gold surface. The triamino acid sequence RGD was added as an example of the inclusion of specific interactions on a nonfouling background, eliminating the need for bioconjugation to synthetic materials such as PEG. This strategy is applicable to any other functional peptide beyond RGD. The concept of this all-in-one natural peptide can be easily adapted to introduce biorecognition, nonfouling, and surface-binding functions into all-natural materials.

EXPERIMENTAL SECTION

Preparation of Peptide SAMs. Peptides were ordered from Synthetic Biomolecules (San Diego, CA) at a purity of >95%. Peptides were synthesized using Fmoc chemistry and purified by reversed-phase high-performance liquid chromatography (RP-HPLC). Gold-coated chips were cleaned by rinsing with Millipore water and ethanol (Decon Laboratories, Inc., King of Prussia, PA) and then drying with filtered air. They were placed in the UV cleaner for 20 min. Cleaned gold chips were incubated in a phosphate buffered saline (PBS) solution (pH 7.4 and ionic strength 150 mM, Sigma-Aldrich, St. Louis, MO) containing 0.14 mM peptide for 24 h. Once removed, the gold chips were rinsed with Millipore water and dried by filtered air. This procedure was followed for all peptide SAM surfaces prepared for SPR, ATR-FTIR, XPS, and cell adhesion experiments.

Protein Adsorption by SPR Sensor. A four-channel SPR sensor was used to measure protein adsorption. Samples were rinsed with Millipore water, dried by filtered air, and mounted on the device. The temperature controller was set to 25 ± 0.01 °C. Protein adsorption was measured by flowing PBS over the SAM at 40 μL/min for 10 min, a 1 mg/mL protein solution of fibrinogen (from bovine plasma, Sigma) or lysozyme (from chicken egg white, Sigma) for 10 min, and finally a PBS rinse for 10 min. The wavelength shift between baselines before protein injection and after rinsing was used to quantify the total amount of protein adsorbed. A reference channel containing a PBS flow was used for each chip to correct for baseline drift. A 1 nm wavelength shift from 750 nm corresponds to 17 ng/cm^2 adsorbed protein.[27] The detection limit for the SPR sensor was 0.3 ng/cm^2.

CD of Peptide Solutions. CD spectra were recorded between 190 and 270 nm (step resolution of 0.2 nm) on 0.1 mg/mL peptide in 10 mM potassium phosphate (J.T. Baker, Austin, TX), 50 mM sodium sulfate (EMD, Darmstadt, Germany) buffer (pH 7.4) at 25 °C using a JASCO J-720 CD spectropolarimeter with an optical cell having a path length of 1.0 mm. Each experiment was repeated three times. Buffer spectra were recorded and subtracted from the sample spectra.

Secondary Structure Simulations. MD simulations were conducted using the GROMACS 4.5.3 simulation engine[28] and the AMBER99sb-ildn force field.[29] Replica exchange with 100 replicas, exchange attempts every 50 fs, and a time step of 2 fs in the NVT ensemble were used for the simulations. The temperature distribution was from 300 to 450 K and can be seen in the Supporting Information. Particle-mesh Ewald sums were used to treat electrostatics.[30] The van der Walls cutoff was 1 nm with an appropriate shifting function. The "v-rescale" thermostat[31], a stochastic thermostat not to be confused with velocity rescaling, was used. The thermostat time constant was 0.5 ps. The simulations were run for 20 ns, and the secondary structure was characterized at the 300 K replica using the DSSP program.[32] The per-residue modes are shown in Figure 4. Further information on the preparation of the systems and information on the Monte Carlo simulations of the proline linker peptide can be found in the Supporting Information.

ATR-FTIR of Peptide SAMs. Peptide SAMs were assembled on gold-coated mica substrates. After incubation, the chips were dried in a desiccator overnight before evaluation by ATR-FTIR. The ATR-FTIR spectra were acquired using Harrick's GATR single-angle reflection accessory in conjunction with a Bruker Tensor spectrometer. Each spectrum was collected with a minimum of 80 scans at a resolution of 4 cm^{-1} and an incident angle of 65°. Optimum contact between the germanium crystal and the sample were maintained throughout measurements. Bare gold on mica was recorded as the background spectrum, which was subtracted from the sample spectra. Three replicates of each SAM were analyzed.

XPS of Peptide SAMs. Peptide SAMs were assembled on gold-coated mica substrates. XPS experiments were performed on a Kratos Axis Ultra DLD spectrometer using a monochromatic Al Kα X-ray source ($h\nu$ = 1486.6 eV) operated at 10 mA and 15 kV. The analysis area was approximately 300 μm × 700 μm. Survey spectra were acquired with an analyzer pass energy of 80 eV. The high-resolution S 2p and C 1s spectra were acquired with an analyzer pass energy of 20 eV. All of the XPS data were acquired at a nominal photoelectron takeoff angle of 0°, where the takeoff angle is defined as the angle between the surface normal and the axis of the analyzer lens. Three spots on two replicates of each SAM were examined. The compositional data are averages of the values determined at each analysis spot.

Cell Seeding of Peptide SAMs. Prior to cell adhesion experiments, samples were sterilized by soaking and rinsing with copious amounts of sterilized PBS. NIH-3T3 fibroblasts (ATCC, Manassas, VA) were plated at 4 × 10^4 cells/mL in 3 mL Dulbecco's Modified Eagle Medium (DMEM) with 10% (v/v) fetal bovine serum and 1% (v/v) penicillin–streptomycin (PS) (Invitrogen Corp, Carlsbad, CA) and incubated for 24 h at 37 °C in 5% CO_2 and 100% relative humidity. The cell seeding density was determined using a hemocytometer. Cell adhesion and morphology were observed under a phase-contrast microscope (Nikon Eclipse TE2000-U). The number of cells adhered was determined by visually counting cells present in at least three microscope images (100× objective magnification).

ASSOCIATED CONTENT

Supporting Information

Simulations and SPR data on the effect of peptide linker length, XPS surface composition data, cell adhesion control experiment, and details of simulation methods. This material is available free of charge via the Internet at http://pubs.acs.org.

AUTHOR INFORMATION

Corresponding Author

sjiang@u.washington.edu

Notes

The authors declare no competing financial interest.

■ ACKNOWLEDGMENTS

This work was made possible by financial support from the National Science Foundation (CBET-0854298) and the Office of Naval Research (N00014-10-1-0600). A.K.N. acknowledges the National Science Foundation for fellowship support. XPS samples were analyzed by the NESAC/BIO facility at the University of Washington (NIH Grant EB-002027). The authors thank Lara Gamble and Jeanette Stein for useful discussions relating to this project.

■ REFERENCES

(1) Chen, S.; Cao, Z.; Jiang, S. *Biomaterials* **2009**, *30*, 5892−5896.
(2) Chen, S.; Zheng, J.; Li, L.; Jiang, S. *J. Am. Chem. Soc.* **2005**, *127*, 14473−14478.
(3) Chelmowski, R.; Köster, D.; Kerstan, A.; Prekelt, A.; Grunwald, C.; Winkler, T.; Metzler-Nolte, N.; Terfort, A.; Wöll, C. *J. Am. Chem. Soc.* **2008**, *130*, 14952−14953.
(4) Bolduc, O. R.; Pelletier, J. N.; Masson, J. F. *Anal. Chem.* **2010**, *82*, 3699−3706.
(5) Statz, A. R.; Meagher, R. J.; Barron, A. E.; Messersmith, P. B. *J. Am. Chem. Soc.* **2005**, *127*, 7972−7973.
(6) Boncheva, M.; Vogel, H. *Biophys. J.* **1997**, *73*, 1056−1072.
(7) Ostuni, E.; Chapman, R. G.; Holmlin, R. E.; Takayama, S.; Whitesides, G. M. *Langmuir* **2001**, *17*, 5605−5620.
(8) Hynes, R. O. *Cell* **2002**, *110*, 673−687.
(9) VandeVondele, S.; Vörös, J.; Hubbell, J. A. *Biotechnol. Bioeng.* **2003**, *82*, 784−790.
(10) Veronese, F. M. *Biomaterials* **2001**, *22*, 405−417.
(11) Perlin, L.; MacNeil, S.; Rimmer, S. *Soft Matter* **2008**, *4*, 2331−2349.
(12) Niu, X.; Wang, Y.; Luo, Y.; Xin, J.; Li, Y. *J. Mater. Sci. Technol.* **2005**, *21*, 571−576.
(13) MacArthur, M. W.; Thornton, J. M. *J. Mol. Biol.* **1991**, *218*, 397−412.
(14) Creighton, T. E. *Science* **1990**, *247*, 1351−1352.
(15) Tsai, W. B.; Grunkemeier, J. M.; Horbett, T. A. *J. Biomed. Mater. Res.* **1999**, *44*, 130−139.
(16) Rohl, C. A.; Strauss, C. E. M.; Misura, K. M. S.; Baker, D. *Methods Enzymol.* **2004**, *383*, 66−93.
(17) Zhang, S.; Yan, L.; Altman, M.; Lässle, M.; Nugent, H.; Frankel, F.; Lauffenburger, D. A.; Whitesides, G. M.; Rich, A. *Biomaterials* **1999**, *20*, 1213−1220.
(18) Lévy, R.; Thanh, N. T. K.; Doty, R. C.; Hussain, I.; Nichols, R. J.; Schiffrin, D. J.; Brust, M.; Fernig, D. G. *J. Am. Chem. Soc.* **2004**, *126*, 10076−10084.
(19) Nam, K. T.; Shelby, S. A.; Choi, P. H.; Marciel, A. B.; Chen, R.; Tan, L.; Chu, T. K.; Mesch, R. A.; Lee, B.; Connolly, M. D.; Kisielowski, C.; Zuckermann, R. N. *Nat. Mater.* **2010**, *9*, 454−460.
(20) Greenfield, N. J. *Nat. Protoc.* **2006**, *1*, 2876−2890.
(21) Woody, R. W. *J. Am. Chem. Soc.* **2009**, *131*, 8234−8245.
(22) Surewicz, W. K.; Mantsch, J. H. H.; Chapman, D. *Biochemistry* **1993**, *32*, 389−394.
(23) Sakurai, T.; Oka, S.; Kubo, A.; Nishiyama, K.; Taniguchi, I. *J. Pept. Sci.* **2006**, *12*, 396−402.
(24) *Infrared Analysis of Peptides and Proteins: Principles and Applications*; Singh, B. R., Ed.; American Chemical Society: Washington, DC, 2000.
(25) Castner, D. G.; Hinds, K.; Grainger, D. W. *Langmuir* **1996**, *12*, 5083−5086.
(26) Herrwerth, S.; Eck, W.; Reinhardt, S.; Grunze, M. *J. Am. Chem. Soc.* **2003**, *125*, 9359−9366.
(27) *Surface Plasmon Resonance Based Sensors*; Wolfbeis, O. S., Homola, J., Eds.; Springer Series on Chemical Sensors and Biosensors, Vol. *4*; Springer: New York, 2006.
(28) Hess, B.; Kutzner, C.; van der Spoel, D.; Lindahl, E. *J. Chem. Theory Comput.* **2008**, *4*, 435−447.
(29) Lindorff-Larsen, K.; Piana, S.; Palmo, K.; Maragakis, P.; Klepeis, J. L.; Dror, R. O.; Shaw, D. E. *Proteins* **2010**, *78*, 1950−1958.
(30) Essmann, U.; Perera, L.; Berkowitz, M. L.; Darden, T.; Lee, H.; Pedersen, L. G. *J. Chem. Phys.* **1995**, *103*, 8577−8593.
(31) Bussi, G.; Donadio, D.; Parrinello, M. *J. Chem. Phys.* **2007**, *126*, No. 014101.
(32) Kabsch, W.; Sander, C. *Biopolymers* **1983**, *22*, 2577−2637.